

Effect of Mesh Size on the Supersonic Viscous Flow Parameters around an Axisymmetric Blunt Body

Rabah Haoui

Abstract—The aim of this work is to analyze a viscous flow around the axisymmetric blunt body taken into account the mesh size both in the free stream and into the boundary layer. The resolution of the Navier-Stokes equations is realized by using the finite volume method to determine the flow parameters and detached shock position. The numerical technique uses the Flux Vector Splitting method of Van Leer. Here, adequate time stepping parameter, CFL coefficient and mesh size level are selected to ensure numerical convergence. The effect of the mesh size is significant on the shear stress and velocity profile. The best solution is obtained with using a very fine grid. This study enabled us to confirm that the determination of boundary layer thickness can be obtained only if the size of the mesh is lower than a certain value limits given by our calculations.

Keywords—Supersonic flow, viscous flow, finite volume, blunt body.

I. INTRODUCTION

THIS article presents a calculation of a viscous flow around an axisymmetric blunt body. In the present work, we employ a numerical technique to simulate the viscous supersonic flow and the boundary layer thickness on the body surface. The gas considered is the air in a standard state composed of 21% of O_2 and 79% of N_2 which is supposed a perfect gas. The free-stream parameters are 170 Pascal and 295K, corresponding at the altitude of 45 Km. thus the vibration and dissociation of molecules are neglected.

The nonlinear partial derivative equations system which governs this flow is solved by an explicit unsteady numerical scheme [1] by the finite volume method [2] and [3]. It is clear that the stationary solution obtained depends on the size of the mesh used in the numerical Discretization [4]. We tested convergence for an inviscid flow by using a refining of grid which will enable us to have the exact solution; after this, we refined again the grid near the wall to determine the boundary layer thickness.

II. GOVERNING OF EQUATIONS

In a Newtonian fluid the viscous stresses are proportional to the rates of deformation. The three-dimensional form of Newton's law of viscosity for compressible flows involves two constants of proportionality, then first dynamic viscosity, μ to relate stresses to linear deformations, and the

second viscosity, λ to relate stresses to the volumetric deformation. The viscous stress components are:

$$\begin{aligned}\tau_{xx} &= 2\mu \frac{\partial u}{\partial x} + \lambda \operatorname{div}(\vec{V}) \\ \tau_{yy} &= 2\mu \frac{\partial v}{\partial y} + \lambda \operatorname{div}(\vec{V}) \\ \tau_{zz} &= 2\mu \frac{\partial w}{\partial z} + \lambda \operatorname{div}(\vec{V}) \\ \tau_{xy} &= \tau_{yx} = \mu \left(\frac{\partial u}{\partial y} + \frac{\partial v}{\partial x} \right) \\ \tau_{xz} &= \tau_{zx} = \mu \left(\frac{\partial u}{\partial z} + \frac{\partial w}{\partial x} \right) \\ \tau_{yz} &= \tau_{zy} = \mu \left(\frac{\partial v}{\partial z} + \frac{\partial w}{\partial y} \right)\end{aligned}$$

Not much is known about the second viscosity λ , because its effect is small in practice. For gases a good working approximation can be obtained by taking the value $= -\frac{2}{3}\mu$.

The Navier-stokes equations in a flux-vector formulation in Cartesian coordinate system is given by

$$\frac{\partial W}{\partial t} + \frac{\partial E}{\partial x} + \frac{\partial F}{\partial y} + \frac{\partial G}{\partial z} = 0 \quad (1)$$

where W, E, F and G are vectors given by

$$\begin{aligned}W &= \begin{pmatrix} \rho \\ \rho u \\ \rho v \\ \rho w \\ \rho e \end{pmatrix} \\ E &= \begin{pmatrix} \rho u \\ \rho u^2 + p - \tau_{xx} \\ \rho uv - \tau_{xy} \\ \rho uw - \tau_{xz} \\ (\rho e + p)u - u\tau_{xx} - v\tau_{xy} - w\tau_{xz} + q_x \end{pmatrix} \\ F &= \begin{pmatrix} \rho v \\ \rho uv - \tau_{xy} \\ \rho v^2 + p - \tau_{yy} \\ \rho vw - \tau_{yz} \\ (\rho e + p)v - u\tau_{xy} - v\tau_{yy} - w\tau_{yz} + q_y \end{pmatrix} \\ G &= \begin{pmatrix} \rho w \\ \rho uw - \tau_{xz} \\ \rho vw - \tau_{yz} \\ \rho w^2 + p - \tau_{zz} \\ (\rho e + p)w - u\tau_{xz} - v\tau_{yz} - w\tau_{zz} + q_z \end{pmatrix}\end{aligned}$$

R. Haoui is with the Mechanical Engineering Department, University of sciences and technology Houari Boumediene, BP32, Al Alia, Algiers, Algeria, (e-mail: haoui_rabah@yahoo.fr).

The heat flux vector q has three components q_x, q_y and q_z given by the Fourier's law of heat conduction relates the heat flux to the local temperature gradient. So

$$q_x = -k \frac{\partial T}{\partial x}, \quad q_y = -k \frac{\partial T}{\partial y}, \quad q_z = -k \frac{\partial T}{\partial z} \quad (2)$$

where k denotes the coefficient of thermal conductivity, it is function of Prandtl number $Pr = 0.75$, viscosity and specific heat.

$$k = Cp \cdot \mu / Pr \quad (3)$$

The energy per unit of mass e is defined as sum of internal energy and kinetic energy such as

$$e = c_v T + \frac{1}{2}(u^2 + v^2 + w^2) \quad (4)$$

III. AXISYMMETRIC FORMULATION

We do not lose general information by seeking the solution at the points of an infinitely small domain Fig. 1. A method developed within the Sinus project of the INRIA Sophia-Antipolis [1] makes it possible to pass from 3D to 2D axisymmetric by using a technique of disturbance of domain. Taking advantage of this finding, here the problem is considered as being axisymmetric.

The system of (1) can be written as:

$$mes(C_{i,j}) \frac{\partial W_{i,j}}{\partial t} + \sum_{a \in \{x, x', y, y'\}} (F_{i,j} \vec{i} + G_{i,j} \vec{j}) \cdot \vec{\eta}_a - H \cdot aire(C_{i,j}) = 0 \quad (5)$$

where $mes(C_{i,j})$ is the measurement (in m^3) of an infinitely small volume of center (i,j) . $aire(C_{i,j})$ is the surface of the symmetry plane passing by the center of elementary volume. $\vec{\eta}_a$ is the integrated normal. The third term of the equation expresses the axisymmetric flow condition. Flows, W , F , G and H this time are given by:

$$W = \begin{pmatrix} \rho \\ \rho u \\ \rho v \\ \rho e \end{pmatrix}$$

$$F = \begin{pmatrix} \rho u \\ \rho u^2 + p - \tau_{xx} \\ \rho uv - \tau_{xy} \\ (\rho e + p)u - u\tau_{xx} - v\tau_{xy} + q_x \end{pmatrix}$$

$$G = \begin{pmatrix} \rho v \\ \rho uv - \tau_{xy} \\ \rho v^2 + p - \tau_{yy} \\ (\rho e + p)v - u\tau_{xy} - v\tau_{yy} + q_y \end{pmatrix}$$

$$H = \begin{pmatrix} 0 \\ -2\tau_{xy} \\ 2p - 2\tau_{yy} \\ -2u\tau_{xy} - 2v\tau_{yy} + 2v\tau_{zz} + 2q_y \end{pmatrix}$$

where

$$\begin{aligned} \tau_{xx} &= 2/3\mu \left(2 \frac{\partial u}{\partial x} - \frac{\partial v}{\partial y} \right) \\ \tau_{xy} &= \tau_{yx} = \mu \left(\frac{\partial u}{\partial y} + \frac{\partial v}{\partial x} \right) \\ \tau_{yy} &= 2/3\mu \left(2 \frac{\partial v}{\partial y} - \frac{\partial u}{\partial x} \right) \\ \tau_{xz} &= \tau_{zx} = 0 \\ \tau_{zz} &= 2/3\mu \left(-\frac{\partial u}{\partial x} - \frac{\partial v}{\partial y} \right) \\ \tau_{yz} &= \tau_{zy} = 0 \end{aligned}$$

IV. DISCRETIZATION IN TIME

The present numerical method is based on an explicit approach in time and space. The step of time Δt is such as:

$$\Delta t_{i,j} = \min \left[\left(\frac{\Delta x \cdot CFL}{\|V\| + a} \right), \left(\frac{(\Delta x)^2 \cdot CFL}{2\mu} \right) \right] \quad (6)$$

The CFL (Courant, Friedrich, Lewis) is a stability factor [5]. V is the velocity of the flow and a the speed of sound. Δx is the small length of the mesh at the same point (i,j) . At each time step and for each point (i,j) , the system of (5) can be written as:

$$W_{i,j}^{n+1} = W_{i,j}^n - \frac{\Delta t_{i,j}}{mes(C_{i,j})} \sum_{a \in \{x, x', y, y'\}} (F_{i,j} \vec{i} + G_{i,j} \vec{j}) \cdot \vec{\eta}_a + \Delta t_{i,j} \frac{aire(C_{i,j})}{mes(C_{i,j})} H_{i,j}^n \quad (7)$$

The choice of the grid plays an important role in determining in the convergence of calculations. Therefore, it is indeed advisable to have sufficiently refine meshes at the places where the gradients of the flow parameters are significantly large.

V. DECOMPOSITION OF VAN-LEER

In this study, the decomposition of Van-Leer [6] is selected, namely a decomposition of flows in two parts f_{VL}^- and f_{VL}^+ . This decomposition must apply to the present two-dimensional problem by calculating the flow within each interface between two cells. Moreover, through this interface, the normal direction is paramount, thus, a change of reference mark is applied to place in the reference mark of the interface and its normal by the intermediary of a rotation \mathbf{R} , Fig. 2.

The vector W_E (variable of Euler) is written W_E^R in the new reference mark

$$W_E^R = \begin{pmatrix} \rho \\ \rho \vec{V}_n \\ \rho e \end{pmatrix} \quad (8)$$

where \vec{V}_n is obtained from \vec{V} , via the rotation \mathbf{R} , in the following way:

$$\vec{V} = \begin{pmatrix} u \\ v \end{pmatrix} \rightarrow \vec{V}_n = \begin{pmatrix} u_n \\ v_n \end{pmatrix} = \begin{pmatrix} \cos \theta & \sin \theta \\ -\sin \theta & \cos \theta \end{pmatrix} \begin{pmatrix} u \\ v \end{pmatrix} \quad (9)$$

where

$$\cos \theta = \frac{\eta_x}{\|\vec{\eta}\|}, \quad \sin \theta = \frac{\eta_y}{\|\vec{\eta}\|} \quad (10)$$

$$\|\vec{\eta}\| = \sqrt{\eta_x^2 + \eta_y^2} \quad (11)$$

The overall transformation \mathbf{R} is written overall

$$\mathbf{R} = \begin{pmatrix} \cos \theta & \sin \theta \\ -\sin \theta & \cos \theta \end{pmatrix} \quad (12)$$

$$\mathbf{R}^{-1} = \begin{pmatrix} \cos \theta & -\sin \theta \\ \sin \theta & \cos \theta \end{pmatrix} \quad (13)$$

Moreover, at each interface $i + 1/2$, two neighbor states i and $i + 1$ are known. Thus, one can calculate the one-dimensional flow F through the interface, total flow $f(W, \eta)$ being deduced from F by applying the opposite rotation, as:

$$f(W, \vec{\eta}) = \|\vec{\eta}\| \cdot \mathbf{R}^{-1}(F(W^R)) \quad (14)$$

This property makes it possible to use only one component of flow $f(F$ for example) to define the decomposition of flow in two dimensions. Moreover, this method is much easy and simple to implement than the decomposition of flow in two dimensions $f = F\eta_x + G\eta_y$.

The expressions of F_{VL}^+ and F_{VL}^- in 1-D, which are those of $F_{VL}^+(W^R)$ and $F_{VL}^-(W^R)$ by rotation \mathbf{R} , where W^R is defined like the transform of W , can be written in the following from:

$$F_{VL}^+(W^R) = \begin{cases} F(W^R)M_n \geq 1 \\ \left(\begin{array}{l} \frac{\rho a}{4} \left(\frac{u_n}{a} + 1 \right)^2 = f_1^+ \\ \frac{f_1^+}{\gamma} [(\gamma - 1)u_n + 2a] \\ f_1^+ \cdot v_n \\ \frac{f_1^+}{2} \left[\frac{((\gamma - 1)u_n + 2a)^2}{\gamma^2 - 1} + v_n^2 \right] \end{array} \right) |M_n| < 1 \\ 0 \quad M_n \leq -1 \end{cases} \quad (15)$$

$$F_{VL}^-(W^R) = \begin{cases} 0 \quad M_n \geq 1 \\ \left(\begin{array}{l} \frac{\rho a}{4} \left(\frac{u_n}{a} - 1 \right)^2 = f_1^- \\ \frac{f_1^-}{\gamma} [(\gamma - 1)u_n - 2a] \\ f_1^- \cdot v_n \\ \frac{f_1^-}{2} \left[\frac{((\gamma - 1)u_n - 2a)^2}{\gamma^2 - 1} + v_n^2 \right] \end{array} \right) |M_n| < 1 \\ F(W^R)M_n \leq -1 \end{cases} \quad (16)$$

where $M_n = u_n/a$, u_n and v_n are the velocity in the reference mark of the interface.

For the viscous terms, we are obliged to use a generalized grid (ξ, η) . Near the wall, ξ and η are respectively tangent and parallel to the wall. The return to the cartesian coordinates is done by an opposite calculation.

VI. BOUNDARY CONDITIONS

Open (far field) boundary conditions give the most serious problems for the designer of general purpose CFD codes. All CFD problems are defined in terms of initial and boundary conditions. It is important to specify these correctly and understands their role in the numerical algorithm. In transient

problems the initial values of all the flow variables need to be specified at all solution points in the flow domain. Since this involves no special measures other than initializing the appropriate data arrays in the CFD code we do not need to discuss this topic further. The present work describes the implementation of the following most common boundary conditions in the discretized equations of the finite volume method: inlet, outlet, wall and symmetry Fig. 1.

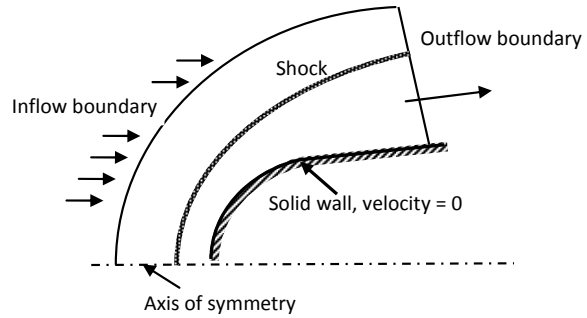


Fig. 1 Computational domain and boundary conditions

A. Inlet Boundary Conditions

At the inlet the Mach number, pressure and temperature are fixed because the flow is supersonic.

B. Body Surface

The no-slip condition for the velocity is usually used at the body surface. The temperature gradient at the wall is zero, in accordance with the Fourier equation of heat conduction in the normal-direction together with the assumption of zero heat flux at the wall. In this study, the wall shear stress is calculated by:

$$\tau_w = \mu \left(\frac{\partial v_t}{\partial n} \right)_{wall} = \mu \frac{v_t}{\Delta n} \quad (17)$$

where

$$V_t = \vec{V} \cdot \vec{t} \quad (18)$$

and

$$\Delta n = \sqrt{\Delta x^2 + \Delta y^2} \quad (19)$$

Here we assume that the coordinate of the unit vector \vec{t} is in the direction of the shear force at the wall and the unit vector \vec{n} is normal at \vec{t} Fig. 2.

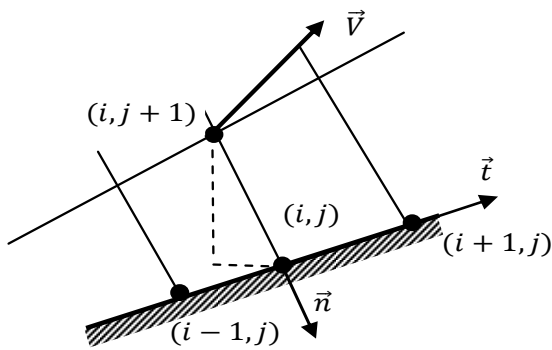


Fig. 2 Grid near the wall

C. Axis of Symmetry

The conditions at axis of symmetry boundary are no flow and no scalar flux across the boundary.

D. Outlet Boundary Conditions

At the exit of the computational domain, the values of the flow parameters are extrapolated from the interior values, including in the boundary layer.

VII. RESULTS AND INTERPRETATIONS

Consider an axisymmetric blunt body defined geometrically by hemisphere as shown in Fig. 3, when the ray is denoted by $r = 4 \text{ cm}$. The computational domain is limited by the blunt body and an ellipse with $a = 1.2 r$ and $b = 1.5 r$. Assume a hypersonic flow-field where the free-stream Mach number equal 6, corresponding to the velocity of 2065 m/s. The configuration is at zero degree angle of attack. The Van Leer flux vector splitting scheme is adapted for this purpose. A (20x100) grid system is created by an elliptic scheme. Note that grid points are clustered near the stagnation region where the flow is expected to be subsonic. In our calculations we used several sizes of grid while starting with that of Fig. 3 (20x100), 20 meshes along the axis and 100 meshes along the wall.

Firstly, one must fix the residue value from which the results remain unchanged. The parameter which interests us much more in this study is the velocity profile in order to capture the boundary layer thickness Fig. 4. We observe that the velocity profile is almost the same when the order of the residue is 10^{-3} to 10^{-6} . In the continuation of our work we stop calculations when the residue equal 10^{-4} . Note that the velocity is calculated paralleling at the wall.

Secondly, one must also fix the size of the grid of the calculation field from which the results remain unchanged, without refinement in the boundary layer. With this intention, one tests six sizes of grid for the same residue Fig. 5. It is observed that the velocity profile starts to be flattened near the wall when the grid is more and more refined. The grid (70x350) is selected since it gives good results and requires less time computing.

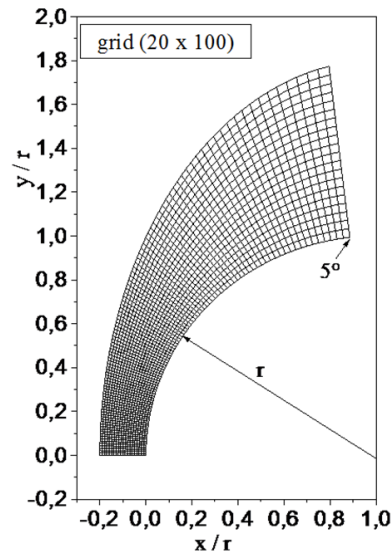
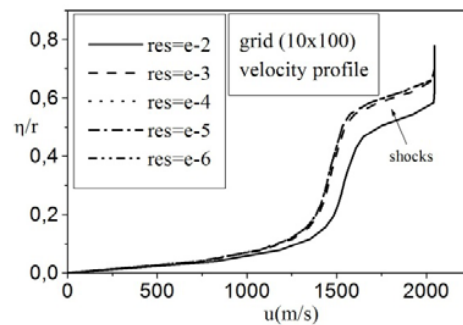
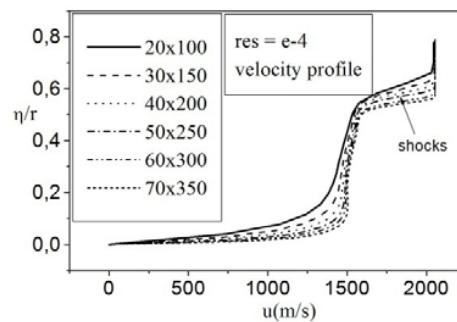


Fig. 3 Grid of solution domain

Fig. 4 Velocity profile with various residues at $x/r = 0.6$ Fig. 5 Velocity profile with various meshes size at $x/r = 0.6$

Another parameter very significant to calculate in this kind of flow, it is that of the stress τ_{xy} . Fig. 6 shows the variation of the stress along the normal of the wall at $x/r = 0.6$ according to the refinement of the grid in the boundary layer. This profile itself converges to the exact solution for a grid of (70x350). It is observed that the intensity of the stress increases quickly while approaching the wall. The viscous stress at the wall can be calculated from the all stresses at the

same point. Fig. 7 shows the variation of the stress τ_{wall} along the wall of the blunt body for different grid.

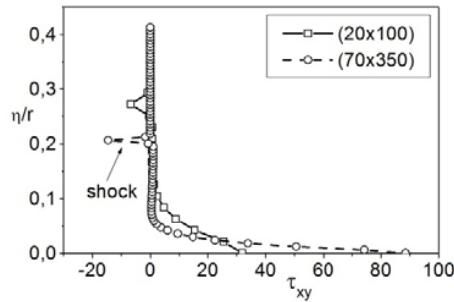


Fig. 6 Stress viscous flow at $x/r = 0.6$

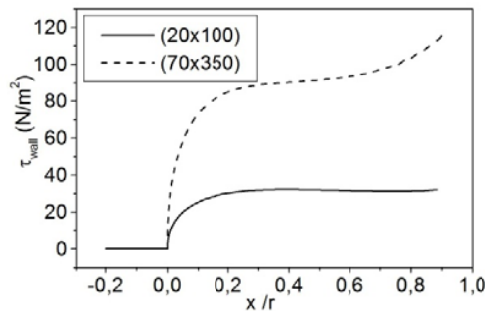


Fig. 7 Stress at the wall for different grids

Concerning the profile of the temperature, it is represented on Fig. 8. The solution also converges to the exact value of the temperature by using refinement (70x350) Fig. 8, the wall of the blunt body is adiabatic and the profile of the temperature is thus perpendicular to the wall. One observes that the wall temperature is 2280K less than 2419K compute by the isentropic equation. The recovery factor at $x/r = 0.6$ is defined as:

$$r = \frac{T_{0w} - T_{\infty}}{T_{0\infty} - T_{\infty}} = 0.935 \quad (21)$$

where, T_{0w} is the adiabatic wall temperature and $T_{0\infty}$ is the isentropic stagnation temperature.

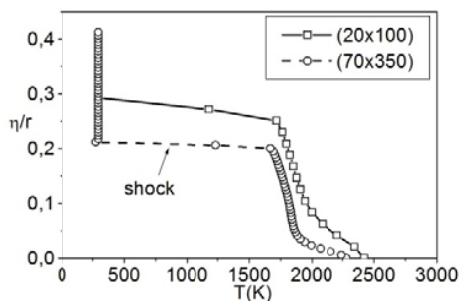


Fig. 8 Static temperature for different grids at $x/r = 0.6$

A Fig. 9 shows the static and stagnation temperatures respectively in the boundary layer. Fig. 10 shows the static and stagnation pressures respectively in boundary layer.

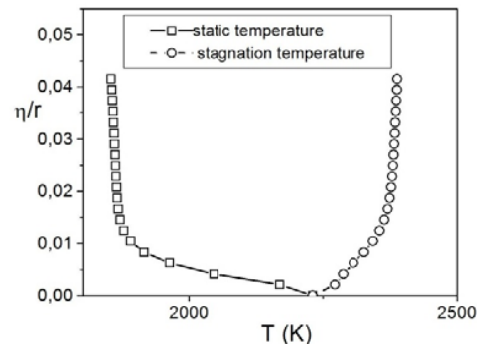


Fig. 9 Temperatures in boundary layer at $x/r = 0.6$

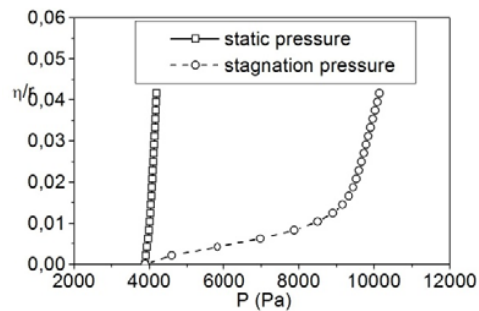


Fig. 10 Pressures in the boundary layer at $x/r = 0.6$

Finally one represents the flow around the blunt body and one compares it with the inviscid flow Figs. 11 and 12.

It is completely clear that the boundary layer influences on the flow parameters.

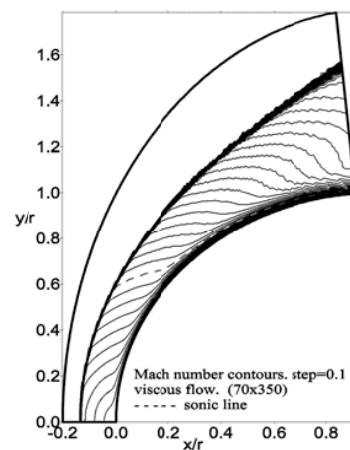


Fig. 11 Mach number contours for viscous flow

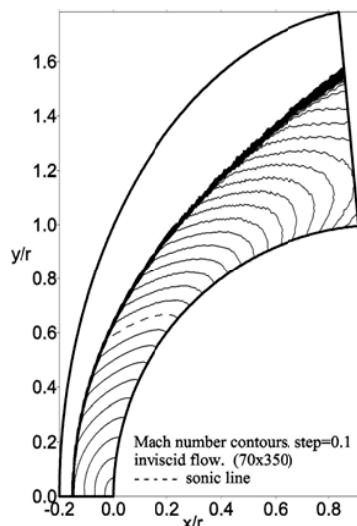


Fig. 12 Mach number contours for inviscid flow

VIII. CONCLUSION

In conclusion, we can confirm that the results obtained in viscous flow depend strongly on the mesh size in numerical calculation. The program converges, certainly, some is the size of the meshes used, but the exact solution is obtained only if the grid, especially near the wall, is refined much more. The approximation by the infinite volumes method with the non-stationary scheme gave good results. Our code is stable, consistent and the solution converges to the exact solution when the grid is very small. The exactitude of our code is carried out by using a mesh size of (350x78) with a residue of 10^{-4} . We saw that the mesh size influences much more on the flow parameters around the blunt body and even on the wall stress.

REFERENCES

- [1] A. Goudjo, J.A. Désidéri, "a finite volume scheme to resolution an axisymmetric Euler equations," Research report INRIA 1005, 1989.
- [2] R. Haoui, A. Gahmousse, D. Zeitoun, "Chemical and vibrational nonequilibrium flow in a hypersonic axisymmetric nozzle," International Journal of Thermal Sciences, article n° 8, volume 40, (2001), pp787-795.
- [3] R. Haoui, "Finite volumes analysis of a supersonic non-equilibrium flow around the axisymmetric blunt body," International Journal of Aeronautical and space Sciences, 11(2), (2010), pp59-68.
- [4] R. Haoui, A. Gahmousse, D. Zeitoun, "Condition of convergence applied to an axisymmetric reactive flow (Condition de convergence appliquée à un écoulement réactif axisymétrique)," 16th CFM, n°738, Nice, France, 2003.
- [5] K. A Hoffmann, "Computational fluid dynamics for engineers," Volume II" Library of congress Catalog, March 1995, ISBN 0-9623731-8-4.
- [6] B. Van Leer, "Flux Vector Splitting for the Euler Equations," Lecture Notes in Physics. 170, (1982), 507-512.